Accepted to Phys. Fluids 10.1063/5.0152446

Gravity currents of viscous fluids in a vertically widening and converging fracture

S. Longo
Department of Engineering and Architecture - Università degli Studi di Parma - Parco Area delle Scienze 181/A - 43124 Parma - Italy[a)]

(Dated: 28 June 2023)

We are investigating flows in the viscous-buoyancy balance regime in a converging channel with an upward increase in width, with the gap of the channel varying according to a $x^k z^r$ power function, being x and z the horizontal and vertical coordinate, respectively, and with $0 < k < 1$ and $0 < r < 1$ in order to be consistent with the model. The fluid rheology is described according to a Ostwald-deWaele model, with a power-law relationship between shear stress and shear rate, and with application for shear-thinning, shear-thickening and, as a special case, Newtonian fluids. While for the case of flow in the direction of widening of the horizontal channel, a self-similar solution of the first kind can be expected, for flow towards the origin, with channel narrowing horizontally, the solution is self-similar of the second kind, with the space and a reduced time coupled in a self-similar independent variable but with an unknown parameter of the transformation group that makes the differential problem invariant. The solution is found in the phase plane by numerical integration of the paths connecting pairs of singular points, separately for the pre-closure phase, in which the current front advances invading the channel, and for the post-closure or levelling phase, in which the fluid has reached the origin and the front no longer propagates, while the level progressively increases cancelling the pressure gradient. Integration is performed with a trial and error procedure by modifying the unknown parameter, generally named eigenvalue and specifically critical eigenvalue when the path has been successfully integrated. The overall effect of an increasing permeability upwards is that of an increase in front speed, with the current profile also becoming locally steeper. The effect of an increase in the fluid-behaviour index is mixed, as it reduces the speed of the front but still increases the steepness of the local current profile. In any case, the model implies that the eigenvalue tends to infinity for $k \to 1$ even in the presence of an increase in vertical permeability ($r > 0$).

I. INTRODUCTION

Numerous environmental flow fields and other related to everyday experience, differ from each other only in scale factors, being intimately related to the same family of differential problems in which, at most, the value of certain parameters varies. Lava flows and honey spreading on a slice of toast share many characteristics and are described by a differential problem of the same nature. What varies most frequently are the initial conditions and boundary conditions, which fortunately are often (not always) forgotten to make way for an evolution dictated only by local conditions or, in any case, oblivious to influences far away in time and space. To this category belong the self-similar solutions of the first and second kind, brought to the fore by Barenblatt[1] with the introduction of the concept of "intermediate asymptotics", i.e. valid not too early nor too late, but only in an intermediate interval. Self-similar solutions are an approximation of the complete solution, with the advantage, however, that the tools at our disposal allow them to be more easily found in place of the complete solution, moreover in analytical form whereas the complete solution can almost always be known in numerical form.

In simple terms, self-similar solutions of the first kind are characterized by the fact that by applying the criteria of dimensional analysis, on the basis of a general principle of covariance, it is possible to reduce the number of variables involved in the description of the physical problem, and it is often possible to define the structure of the solution as a power-function; this is the first step in transforming, for example, partial derivative problems into ordinary derivative problems, with all the advantages that this entails[2,3]. A more rigorous definition specifies that it is possible to identify a group of transformations with one or more known parameters (Lie group) that makes the differential problem invariant: the problem can be rewritten with a number of variables reduced by a value equal to the number of parameters in the transformation group.

In other cases, we do not have enough information to analytically identify the transformation group, but only its structure except for one parameter. This leads to self-similarities of the second kind, in which the parameter is a part of the solution and is called an eigenvalue. The most favourable case is that the solution leads to a single eigenvalue, instead of a discrete set or spectrum of eigenvalues.

Gravity currents admitting second kind self similar solutions have been studied by several Authors[4–10]. Zheng *et al.* (2014)[11] extended the interpretation of the effects of heterogeneity on second-kind self-similar solutions, with a further extension in Zheng *et al.* (2015)[12], where a permeable substrate was also included.

[a)] https://sandro.longo.unipr.it/

In parallel, the analysis was extended to the case of non-Newtonian power-law fluids[13,14], including both propagation in converging channels in Hele-Shaw similarity, and circular symmetrical currents with flow towards the origin. The latter refer to a flow field dominated by vertical rather than horizontal dynamics. The review in Gratton[15] and in Zheng & Stone[16] provide a detailed overview of the most relevant and of some recent contributions.

One flow configuration that has apparently been left out until now is the flow of gravity currents in converging channels with increasing permeability in the vertical direction. This is equivalent to a fracture with a change in width in the horizontal direction but also in the vertical direction, and can be traced back to the case of flow in porous media with a change in permeability/porosity in the two main directions of flow[11,14,17]. For the case of flow in the direction of the horizontally widening channel, we expect a self-similar solution of the first kind, since it is possible to use the criteria of dimensional analysis to determine analytically the transformation that leaves the differential problem invariant[3].

The present work focuses on the theoretical analysis of this specific configuration and flow advancing towards the origin, also including non-Newtonian power-law fluids, in a context where a self-similarity of the second kind is expected.

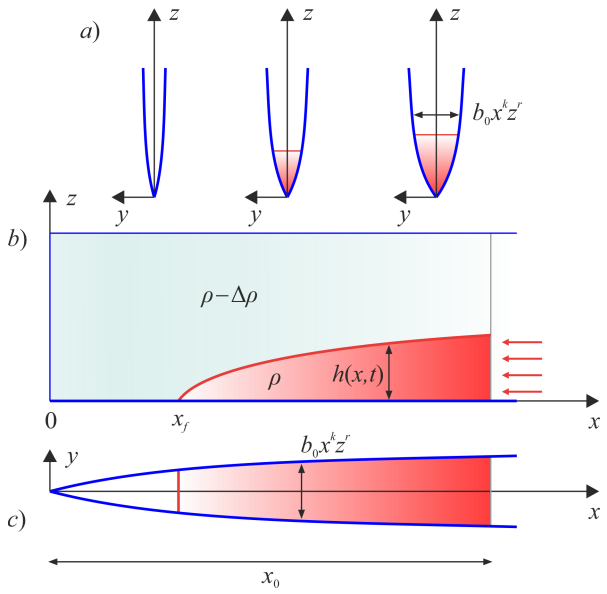

FIG. 1. Horizontal channel with varying width in the horizontal and in the vertical, $b_0x^kz^r$. A converging gravity current in viscous-buoyancy balance propagates toward the origin, with the instantaneous front position x_f and with $x_f \equiv x_0$ the front position at time $t = 0$.

II. THEORY

A. The formulation of the model

We are considering a gravity current of a viscous fluid, described by a Ostwald-deWaele (OdW) model[18,19], propagating towards the origin $x = 0$, in the direction of negative x in a channel of variable cross-section. The OdW model in one dimension reads

$$\tau = \mu_0|\dot\gamma|^{n-1}\dot\gamma, \tag{1}$$

where τ is the tangential stress and $\dot\gamma$ is the strain rate. The consistency index μ_0 is a viscosity-like parameter, and the fluid behaviour index n controls the extent of shear-thinning ($n < 1$) or shear-thickening ($n > 1$), with $n = 1$ corresponding to a Newtonian fluid. The channel has a width varying in the horizontal and in the vertical direction, $b(x, z) = b_0x^kz^r$, where $[b_0] = L^{1-k-r}$, $0 < k < 1$, and $0 < r < 1$. The current evolves toward the origin, with a negative horizontal velocity, by assuming that (i) hydrostatic pressure distribution holds; (ii) the dynamics is in the horizontal, with $\tau_{yx} \gg \tau_{xz}$ and negligible τ_{yz}, and we are in narrow current configuration; no slip at the side wall at $y = \pm b/2$ and null shear stress at $y = 0$; (iv) surface tension has negligible effects and no fingering at the interface with the ambient fluid, and (v) the ambient fluid has a negligible role and does not interact with the main current. Some of these conditions are met in only part of the domain. For example, the surface tension is considered negligible when the smallest dimension of the current (generally, the average width, coincident with the average width of the fracture) is greater than the capillary length[11] equal to $\sqrt{\sigma/(\Delta\rho\, g)}$, where σ is the surface tension, $\Delta\rho \equiv \rho_c - \rho_a$ is the density difference between the intruding current and the ambient fluid and g is gravity.

We are in the condition that we can neglect the vertical velocity and use the lubrication approximation, with an essentially one-dimensional flow field everywhere except near the front of the current, where the capillary length may be locally important and where the tangential stresses field is more varied than in the body of the current. With an analysis of the orders of magnitude of the different terms, it turns out that the validity conditions of the lubrication approximation are: $|\mathrm{d}b/\mathrm{d}x| \ll 1$, $\mathrm{d}h/\mathrm{d}x \ll 1$ and an aspect ratio $b(x_f)/x_f \ll 1$. It is also requested that $0 < k < 1$ and $0 < r < 1$ in order to have an average aspect ratio not increasing with x. The balance is between viscous force and pressure gradient, leading to:

$$\frac{\partial\tau_{yx}}{\partial y} + \frac{\partial p}{\partial x} = 0 \rightarrow \frac{\partial}{\partial y}\left[\mu_0\left(\frac{\partial u}{\partial y}\right)^n\right] = \Delta\rho\, g\frac{\partial h}{\partial x}, \tag{2}$$

where $h(x, t)$ is the current depth. This is an approximation with negligible inertial terms and in the hypothesis that the dominant velocity variation is in the y direction. Integrating we calculate:

$$u(x,y,z,t) = -\mathrm{sgn}\left(\frac{\partial h}{\partial x}\right)\left|\frac{\partial h}{\partial x}\right|^{1/n}\left(\frac{\Delta\rho\, g}{\mu_0}\right)^{1/n}\frac{n}{n+1}\left[\left(\frac{b_0 x^k z^r}{2}\right)^{1+1/n} - |y|^{1+1/n}\right],\ 0\le z\le h,\ |y|\le\frac{b_0 x^k z^r}{2}, \quad (3)$$

where the no-slip condition at $y = \pm(b_0/2)x^k z^r$ and the null stress condition at $y = 0$ have been used.

The stream-wise horizontal velocity of the current averaged over the cross-section is

$$\overline{u}(x,t) = -\mathrm{sgn}\left(\frac{\partial h}{\partial x}\right)\left(\frac{b_0 x^k}{2}\right)^{(n+1)/n}\frac{n^2(r+1)}{(2n+1)[r(2n+1)+n]}\left(\frac{\Delta\rho\, g}{\mu_0}\right)^{1/n} h^{r(n+1)/n}\left|\frac{\partial h}{\partial x}\right|^{1/n}. \quad (4)$$

For an incompressible fluid in a monodimensional current, the mass conservation is

$$\frac{\partial\Omega}{\partial t} + \frac{\partial\Omega\overline{u}}{\partial x} = 0, \quad (5)$$

where Ω is the cross-section area and $\Omega\overline{u}$ is the flow rate. The cross-section area is $\Omega = b_0/(r+1)x^k h^{r+1}$ and the flow rate is $Q \equiv \Omega\overline{u} = b_0/(r+1)x^k h^{r+1}\overline{u}(x,t)$. For simplicity, in the following we eliminate the overline on u. Substituting in eq.(5), the mass conservation reads

$$\frac{\partial h^{r+1}}{\partial t} + \frac{1}{x^k}\frac{\partial(x^k h^{r+1}u)}{\partial x} = 0. \quad (6)$$

The differential problem solution requires the specification of boundary and initial conditions. If the domain occupied by the current were limited, we could impose mass conservation by possibly including an input or output flow rate. On the other hand, we are in the condition in which the extent of the current is such that it loses the memory of the boundary conditions; this can lead to the solution becoming self-similar, but there is a loss of information that uniquely characterizes the solution. A quick calculation indicates that a self-similar solution of the first kind is not possible, since at least one other equation is missing to identify the transformation group in which the differential problem is invariant. To adimensionalize the problem, instead of using scales "external" to the flow field we consider "internal" scales, as follows. We let

$$u(x,t) = \frac{x}{t_r}U(x,t_r), \quad (7a)$$

$$h(x,t) = \left(\frac{2}{b_0}\right)^{(n+1)F_1}\left[\frac{(2n+1)[r(2n+1)+n]}{n^2(r+1)}\right]^{nF_1}\left(\frac{\mu_0}{\Delta\rho\, g}\right)^{F_1}\frac{x^{(n+1)(1-k)F_1}}{t_r|t_r|^{nF_1-1}}H(x,t_r), \quad F_1 = 1+r(n+1), \quad (7b)$$

where H and U are dimensionless and $t_r = t_c - t$, being t_c the closure time, i.e. the time required for the current, starting with the front at x_0, to reach the origin. This choice of a time relative to closure time makes it possible to analyse separately the initial phase of current evolution, or "pre-closure" in which $t_r > 0$ and $x_f \to 0$, from the subsequent "post-closure" or "levelling" phase, with $t_r < 0$ and with the current gradually increasing in level having already reached the origin and $x_f = 0$.

Substituting eqs.(7a–7b) into eqs.(4–6) yields

$$U|U|^{n-1} + \frac{(n+1)(1-k)}{F_1}H|H|^{F_1-1} + H|H|^{F_1-2}x\frac{\partial H}{\partial x} = 0, \quad (8a)$$

$$t_r\frac{\partial(H|H|^r)}{\partial t_r} - \frac{n(r+1)}{F_1}H|H|^r - \frac{[n(1-k)+2F_1]}{F_1}H|H|^r U - x\frac{\partial(H|H|^r U)}{\partial x} = 0. \quad (8b)$$

It is a nonlinear system of partial derivative equations in the two dependent dimensionless variables H and U

and the independent dimensional variables x and t_r. We introduce the self-similar variable $\xi = x/(lt_r|t_r|^{\delta-1})$ that couples x and t_r, l being a dimensional parameter having dimensions $[l] = LT^{-\delta}$. Inserting the similarity variable into eqs.(8a–8b) gives

$$U\,|U|^{n-1} + H|H|^{F_1-2}\xi H' + \frac{(n+1)(1-k)}{F_1} H|H|^{F_1-1} = 0, \tag{9a}$$

$$\delta(r+1)\xi H' + \frac{n(r+1)}{F_1} H + (r+1)U\xi H' + H\xi U' + \frac{[n(1-k)+2F_1]}{F_1} HU = 0, \tag{9b}$$

where the prime indicates the derivative with respect to ξ and where the variable t_r does not appear explicitely. Eliminating ξ from the two equations results in

$$\frac{\mathrm{d}H}{\mathrm{d}U} = \frac{H|H|^{2F_1-2}[(n+1)(1-k)H|H|^{F_1-1} + F_1 U\,|U|^{n-1}]}{H|H|^{F_1-1}[(k+1)F_1U - (n+1)(1-k)(r+1)\delta + n(r+1)] - (r+1)(U+\delta)F_1U\,|U|^{n-1}}, \tag{10a}$$

$$\frac{\mathrm{d}\ln\xi}{\mathrm{d}H} = -\frac{F_1}{H|H|^{F_1-2}F_1U\,|U|^{n-1} + (n+1)(1-k)H|H|^{2F_1-2}}. \tag{10b}$$

It is an autonomous system of ordinary differential equations (ODE), lacking, for the moment, the boundary conditions. The solutions are represented by paths in the phase space $U - H$. Not all paths are representative of the physical behaviour of a current, but only some of them connecting two singular (or critical) points.

The singular points correspond to the simultaneous zeros of numerator and denominator of eq.(10a) , with a further singular point (point C, see below) corresponding to $\mathrm{d}U/\mathrm{d}H = 0$ for $H \to -\infty$. Amongst the singular points, only points O, A, B and C in the following list are of interest:

$$\mathrm{O} : (H,U) \equiv (0,0), \tag{11a}$$

$$\mathrm{A} : (H,U) \equiv (0,-\delta), \tag{11b}$$

$$\mathrm{B} : (H,U) \equiv \left(\left[\frac{n(r+1)}{n(1-k)+2F_1}\right]^{n/F_1}\left[\frac{F_1}{(n+1)(1-k)}\right]^{1/F_1}, -\frac{n(r+1)}{n(1-k)+2F_1}\right), \tag{11c}$$

$$\mathrm{C} : (H,U) \equiv \left(-\infty, \frac{(r+1)[(n+1)(1-k)\delta - n]}{(k+1)F_1}\right). \tag{11d}$$

The origin O corresponds to null velocity and height at $t_r = 0$ (and to $\xi \to \infty$); point A corresponds to the moving front where $h(x_f(t),t) = 0$, with x_f the front position and $x_f(t=0) = x_0$ (and to $\xi = \xi_f$); point B from an analytic point of view corresponds to the condition $\mathrm{d}^2H/\mathrm{d}U^2 \equiv \mathrm{d}H/\mathrm{d}U = 0$, but it is unphysical since the solution near it evolves like a spiral which indicates an oscillatory behavior of the physical variables u and h, not observed; point C represents the asymptotic flow condition during levelling (it also corresponds to $\xi = 0$). For $n = 1$ and $r = 0$ point B corresponds to the value given in[11], where n in[11] corresponds to our k. For $r = 0$ points O, A, B, and C correspond to the points in[14].

The expansion about the origin O, yields

$$U \approx -\left[\frac{\delta(1-k)(n+1) - n}{F_1\delta}\right]^{1/n} H|H|^{F_1/n-1}; \tag{12}$$

the expansion about the front of the current A, yields

$$U \approx \left[\frac{[(1-k)n+2nr+2(1+r)]\delta - n(1+r)}{F_1(1+r)\delta^n}\right] H^{F_1} - \delta; \tag{13}$$

the asymptotic expression for $H \to -\infty$ (point C) gives

$$U \approx U_C + \frac{U_C^{2-n}(1-k)(n+1)(3F_1-2)}{(1+r)(U_c+\delta)F_1}\frac{1}{H|H|^{3F_1-3}}, \tag{14}$$

where U_C is the coordinate of the singular point C. The description of the behaviour of the solution near the singular points, suggests that the pre-closure current evolution is described by an integral curve joining A and O, the post-closure evolution by a curve joining O and C.

B. Integration of the model and numerical results

We used Mathematica[20] for numerical integration in the pre-closure time interval ($t < t_c$) by adopting eq.(10a), starting nearby the origin O and assuming that $U = -\epsilon$ with the local expansion for H computed by inverting eq.(12), with $\epsilon = 10^{-5}$, and computing $H(U)$ in the interval $U \in [-\delta, -\epsilon]$. An initial value of δ was chosen, with iterative modifications of this value and stop criterion when $H(-\delta) < 10^{-3}$. The computed eigenvalues, named critical eigenvalues δ_c, are listed in table I of Appendix A.

The post-closure interval ($t > t_c$) evolution has been integrated with the same equation (10a) used for the pre-closure interval, but starting nearby point C where $U = U_C - \epsilon$, with the expansion for H obtained by inverting eq.(14), again with $\epsilon = 10^{-5}$, and computing $H(U)$ in the interval $U \in [\epsilon, U_C - \epsilon]$. No iteration was required since the value of δ_c was already known.

Figure 2ab shows the phase portrait of eq.(10a) with the trajectories of a Newtonian current for the critical eigenvalue $\delta_c = 1.74581$ for $r = 0.1$, $k = 0.6$ and $\delta_c = 1.85331$ for $r = 1$, $k = 0.6$. Continuous and dash dotted curves describe the pre-closure and post-closure phases, respectively. The pattern is similar but with the shape of the curve during pre-closure with greater steepness at the front (point A) for the case of $r = 1$, compared to $r = 0.1$.

Figure 3ab shows the heteroclinic trajectories connecting: i) point A and point O (continuous curves, pre-closure) and ii) point O and point C (dashed curves, post-closure or levelling) for $n = 0.7, 1, 1.5$, $k = 0.6$ and increasing r values. The pattern is distinctly different for increasing r, but the shape is rather similar for fluids with different values of the fluid behaviour index n. The results for larger values of k do not change significantly the pattern (not shown).

Figure 4 shows the eigenvalues as a function of r for two different k and three different n. The definition of the front speed in dimensional variables gives

$$u_f = -\frac{x_f}{t_c - t}\delta_c, \tag{15}$$

which can also be expressed as

$$u_f = -\frac{x_0}{t_c}\delta_c\left(1 - \frac{t}{t_c}\right)^{\delta_c - 1}. \tag{16}$$

The acceleration of the front is

$$a_f = \frac{x_0}{t_c^2}\delta_c(\delta_c - 1)\left(1 - \frac{t}{t_c}\right)^{\delta_c - 2}, \tag{17}$$

which is always positive (hence, reduces the negative front speed) since $\delta_c > 1$, and is decreasing/constant/increasing in time for $\delta_c \gtreqless 2$; in the last case, the acceleration approach $+\infty$ for $t \to t_c$. The δ_c value generally increases with r, which means that the current front advances with a higher speed the greater the increase in permeability upwards, and even greater for shear-thinning fluids than for shear-thickening fluids. Faster convergence of the channel (higher value of k) again increases the speed of the front. The variation is most evident for larger values of r. Shear-thickening fluids and for $k = 0.6$ experience an initial reduction of δ_c for r increasing from $r = 0$ (uniform permeability in vertical), due to an interplay between rheology and cross-section geometry.

Once the function $H(U)$ has been computed, the independent similarity variable ξ can be computed by first mapping the domain of varying size $\xi \in [\xi_f, \infty]$ into $\xi/\xi_f \in [1, \infty]$, then integrating eq.(10b) starting from the front of the current A with the boundary condition $\xi/\xi_f|_{U=-\delta_c} = 1$, equivalent to $\mathrm{d}\ln(\xi/\xi_f)|_{U=-\delta_c} = 0$. The origin O is reached for $U \to 0$ at $\xi/\xi_f \to \infty$.

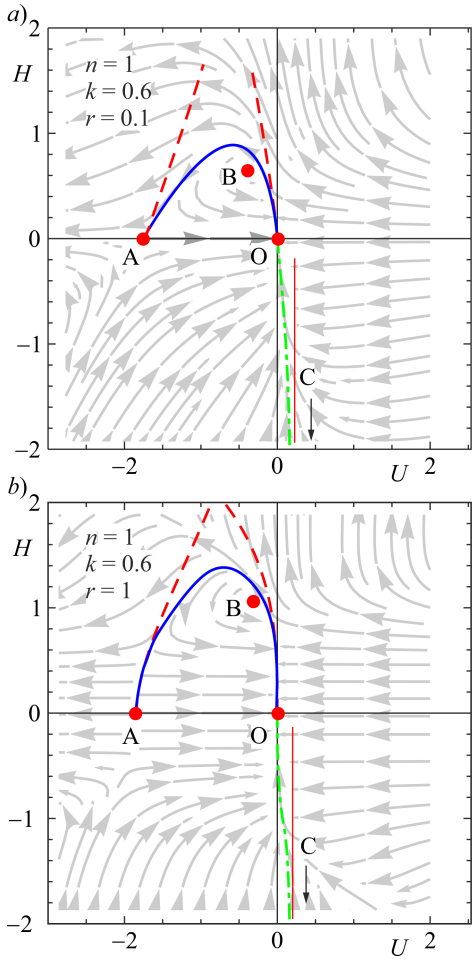

FIG. 2. Converging gravity current in a channel of width $b = b_0 x^k z^r$. Phase portrait of (10a) for $n = 1$ (Newtonian fluid), $k = 0.6$, *a*) $r = 0.1$ with $\delta_c = 1.74581$, and *b*) $r = 1$ with $\delta_c = 1.85331$. The continuous blue curve refers to the pre-closure phase, the dash-dotted green curve refers to the post-closure (levelling) phase, the red vertical line indicates the asymptote in the levelling phase, the red dashed curves are the approximate solutions about points O and A.

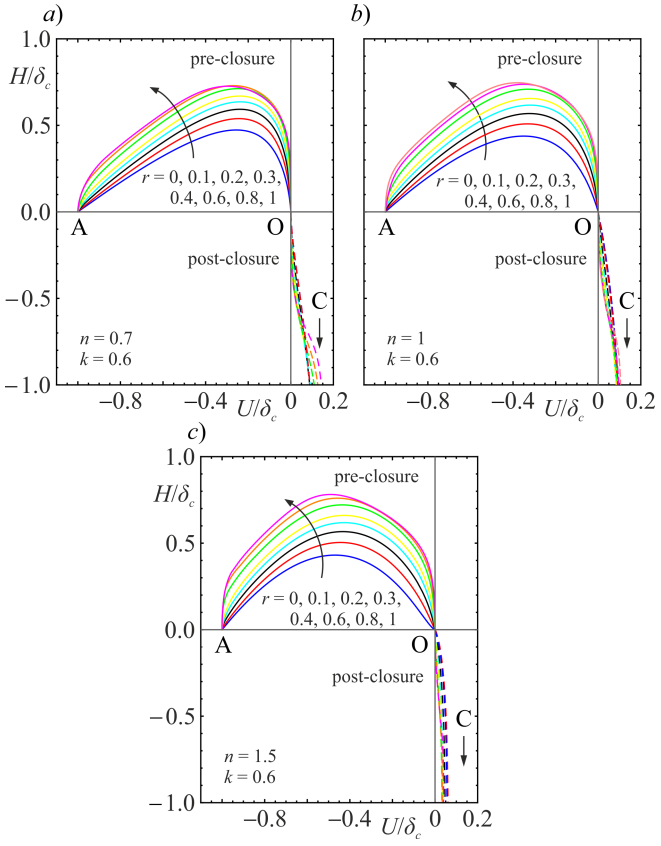

FIG. 3. Converging gravity current in a channel of width $b = b_0 x^k z^r$. Shape of the heteroclinic trajectories in rescaled coordinates for $k = 0.6$ and increasing r for (*a*) $n = 0.7$ (shear-thinning fluid), *b*) for $n = 1$ (Newtonian fluid), and *c*) for $n = 1.5$ (shear-thickening fluid). Continuous curves refer to pre-closure, dashed curves to post-closure (levelling) phase.

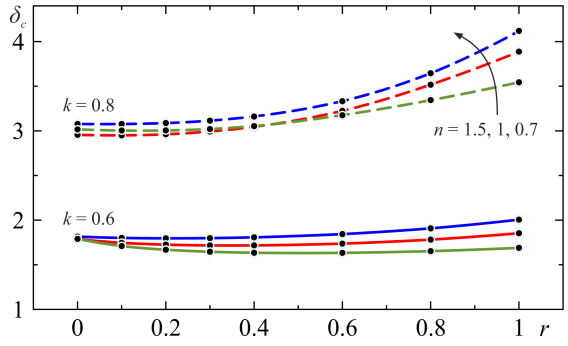

FIG. 4. Converging gravity current in a channel of width $b = b_0 x^k z^r$. Eigenvalues representing the exponent of the similarity variable $\xi = x/[l(t_c - t)^{\delta_c}]$ for fluids with different flow behaviour index n, in a channel with horizontal convergence parameter $k = 0.6, 0.8$ and for increasing vertical divergence parameter r.

A similar approach is adopted for the post-closure phase, when the front of the current has reached the origin and a progressive levelling occurs (not shown).

Figure 5abc shows the current depth and velocity in the pre-closure for different values of the fluid behaviour index n, for $k = 0.8$ and for increasing value of the parameter r. Visualisations are not easy to interpret as dimensionless variables scale nonlinearly with distance from the origin. For example, the presence of a maximum does not indicate the reversal of the gradient of the dimensional height of the current, which must be positive everywhere. However, we can grasp some salient aspects. The increase in upward permeability favours steeper wavefronts, the higher the fluid behaviour index and the faster the horizontal convergence (not shown). The average horizontal velocity, equal to $-\delta_c$ at the front, increases faster for increasing r (and for increasing k, not shown)

C. Numerical study of the pre-closure

A possible validation of the self-similar solution consists of direct numerical integration of the mass conservation and momentum balance equations. Note that this is not a verification of the goodness of the physical model, but only a validation of the goodness of the semi-analytical results obtained in the phase space. By inserting eq.(4) into eq.(6) and selecting the following velocity and time scales:

$$u^* = \frac{n^2(r+1)}{(2n+1)[(2n+1)r+n]} \left(\frac{h^*}{L}\right)^{1/n} \left(\frac{\Delta\rho g}{\mu_0}\right)^{1/n} \left(\frac{b_0 h^{*r} L^k}{2}\right)^{1/n+1}, \quad t^* = \frac{L}{u^*}, \tag{18}$$

where L and h^* are the horizontal and vertical length scales, respectively, the evolution equation of the current height in non dimensional form is

$$\frac{\partial \tilde{H}^{r+1}}{\partial t} = \frac{1}{X^k}\frac{\partial}{\partial X}\left[X^{2k+k/n}\tilde{H}^{2r+1+r/n}\frac{\partial \tilde{H}}{\partial X}\left|\frac{\partial \tilde{H}}{\partial X}\right|^{1/n-1}\right], \tag{19}$$

where $X = x/L$ and $\tilde{H} = h/h^*$. For the simple case of a constant volume, the integral mass conservation in dimensional form is

$$\int_{x_f}^{L} \frac{b_0}{r+1} x^k h^{r+1}\,\mathrm{d}x = V_0, \tag{20}$$

where V_0 is the volume of fluid; the corresponding dimensionless formulation reads

$$\int_{X_f}^{1} X^k \tilde{H}^{r+1}\,\mathrm{d}X = 1, \tag{21}$$

where the vertical length scale becomes

$$h^* = \left[\frac{(r+1)V_0}{b_0 L^{k+1}}\right]^{1/(r+1)}. \tag{22}$$

The boundary conditions are

$$\tilde{H}(X_f) = 0, \quad \left.\frac{\partial \tilde{H}}{\partial X}\right|_{X=1} = 0. \tag{23}$$

It is advantageous to map the time variable domain $[X_f, 1]$ into a fixed domain $[0, 1]$ (see[21]) by introducing the following transformation:

$$Y = \frac{1-X}{1-X_f(T)} \quad 0 < Y < 1. \tag{24}$$

With this transformation, we eliminate some problems arising in a variable domain of integration and simplify the identification of the updated position of the front of the current. Since $\tilde{H}(Y(X,T),T)$, it results:

$$\left.\frac{\partial \tilde{H}}{\partial T}\right|_X = \left.\frac{\partial \tilde{H}}{\partial T}\right|_Y + \left.\frac{\partial \tilde{H}}{\partial Y}\right|_T \frac{\partial Y}{\partial T}, \quad \left.\frac{\partial \tilde{H}}{\partial X}\right|_T = \left.\frac{\partial \tilde{H}}{\partial Y}\right|_T \frac{\partial Y}{\partial X}, \tag{25}$$

where the subscript indicates the constant independent variable. Eq.(19) becomes

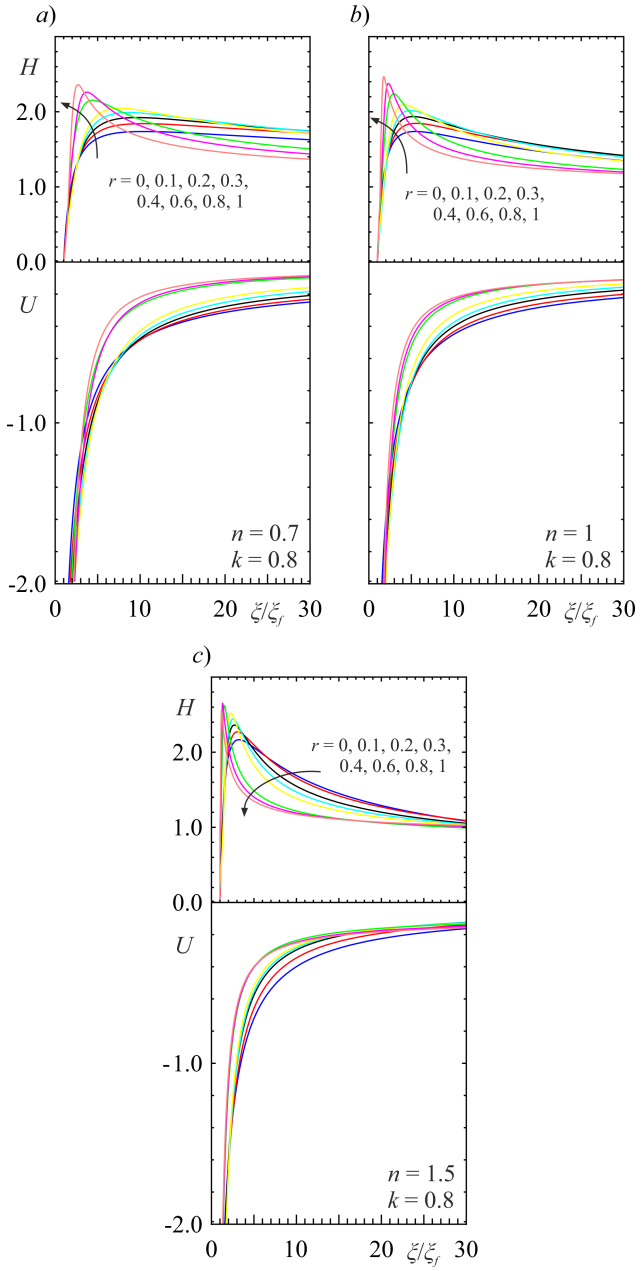

FIG. 5. Current shape profiles and velocity profiles in the pre-closure phase for $k = 0.8$, $r = 0, 0.1, 0.2, 0.3, 0.4, 0.6, 0.8, 1$, a) for shear-thinning fluid with $n = 0.7$, b) for Newtonian fluid with $n = 1$, and c) for shear-thickening fluid with $n = 1.5$.

$$\frac{\partial \tilde{H}^{r+1}}{\partial T} = \frac{Y\dot{X}_f}{1-X_f}\frac{\partial \tilde{H}^{r+1}}{\partial Y} + \frac{1}{[1-Y(1-X_f)]^k}\frac{1}{(1-X_f)^{1/n+1}}\frac{\partial}{\partial Y}\left([1-Y(1-X_f)]^{2k+k/n}\tilde{H}^{2r+1+r/n}\frac{\partial \tilde{H}}{\partial Y}\left|\frac{\partial \tilde{H}}{\partial Y}\right|^{1/n-1}\right), \tag{26}$$

where $\dot{X}_f$ is the front speed. The integral mass continuity eq.(21) becomes:

$$(1-X_f)\int_0^1 [(1-Y(1-X_f)]^k \tilde{H}^{r+1}\mathrm{d}Y = 1, \tag{27}$$

and the boundary conditions become

$$\tilde{H}(1) = 0, \quad \left.\frac{\partial \tilde{H}}{\partial Y}\right|_{Y=0} = 0. \tag{28}$$

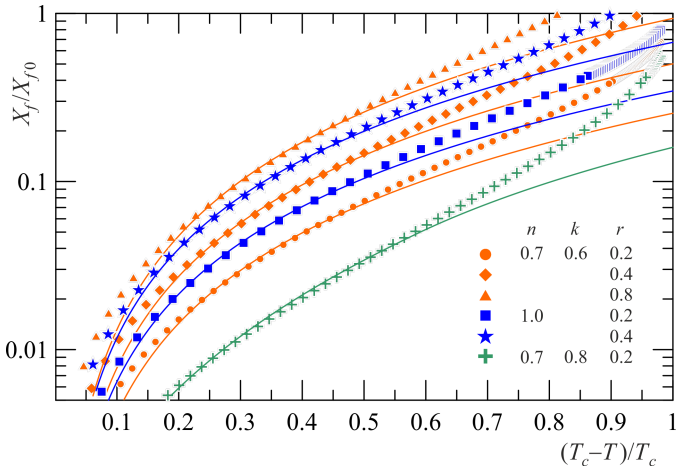

FIG. 6. Comparison of the front position between the predictions of self-similar theory (curves) and numerical simulation (symbols). Note that the vertical scale is logarithmic to better highlight the behaviour near closure, and that the results of different simulations have been translated in the vertical for an easy visualization.

Numerical integration is performed with an explicit predictor-corrector scheme on a staggered grid, with the non-linear terms calculated at intermediate points, starting with an initial condition of the type

$$\tilde{H}(Y,0) = a(1-Y^s), \tag{29}$$

where a and s are dimensionless coefficient. The initial front speed is assumed equal to the velocity of the current in the front cell, computed as

$$\dot{X}_f\Big|_{T=0} = -\frac{\tilde{H}^{r+r/n}}{(1-X_f)^{1/n}} X_f^{k+k/n} \frac{\partial \tilde{H}}{\partial Y} \left|\frac{\partial \tilde{H}}{\partial Y}\right|^{1/n-1}. \tag{30}$$

At each step, we iteratively calculate the updated value of X_f from eq.(27) and then the updated front speed as $\dot{X}_f = (X_{f-new} - X_{f-old})/\mathrm{d}T$. A sensitivity analysis showed that a grid of 200 points guarantees grid-independent results, with an initial integration interval of $\mathrm{d}T = 10^{-5}$ progressively increased at a later stage of propagation of the current.

Figure 6 shows the comparison between the self-similar theory and numerical simulation. Note that in the initial phase the results are divergent, while after a certain time interval the self-similar regime is established with a good overlap between the self-similar solution and the numerical simulation. Note also how in the terminal phase there is a slight new difference between the two solutions of the differential problem.

III. SUMMARY AND CONCLUSION

We conducted an analysis of gravity currents advancing towards the origin in a channel, or fracture, of varying width and converging, with an upward increase in permeability. Previous analyses, conducted for both Newtonian fluids and more generically power-law fluids, had led to a self-similar solution of the second kind, also experimentally validated[6,11,14].

Here we have extended the analysis to the case of heterogeneity in the vertical direction, which appears representative of many real situations. The method adopted is the search for integral paths in phase space, capable of joining two singular points representing the front and an origin at an indefinite distance, in the pre-closure phase, and the origin and an asymptotic point corresponding to the levelling, in the post-closure phase. These paths were integrated numerically by introducing a parameter that is part of the solution, referred to as the eigenvalue. The value of the eigenvalue that allows joining the two points is named critical eigenvalue.

From a numerical point of view, instabilities occur for $r \approx 1$. Numerical instability is often an indication of physical instability, assuming the model is adequately representative of the physical process. The approach of the present analysis has been experimentally validated for simpler geometries, but the condition of vertically increasing permeability will require future experimental verification. As is always the case when handling self-similar solutions, there remains the problem of determining what is the range of validity of the solution[22], which although arising from the essential aspects of the problem, and thus being strongly based on the physics of the problem, may be obscured by the initial and boundary conditions in the initial phase, as well as by the amplification of perturbations in the terminal phase. In the most unlucky cases, self-similar solutions either find no space between the two phases, which overlap, or are so unstable that they evolve rapidly without trace. This definitely requires experimental validation although the numerical integration of the differential problem shows a good overlap with the self-similar solution.

The critical eigenvalue for the converging channel flow is influenced by both the convergence parameter k (higher eigenvalues for increasing k) and the vertical divergence parameter r (generally increasing eigenvalues for increasing r). The nature of the fluid (flow behaviour index n) influences the flow regime much less than the geometry of the cross-section. Although no analytical limit values of the eigenvalue have been found, the critical eigenvalue grows rapidly as $k \to 1$ increases, apparently unlimited.

A possible extension of the analysis is to include a drainage at the bottom, in order to reproduce the competition between bottom filtration and current advancement in an anisotropic domain.

TABLE I. Eigenvalues computed for converging flow in a channel of width $b = b_0 x^k z^r$ for different values of k, r and of fluid behaviour index n.

	$k = 0.6$			$k = 0.8$		
r	$n = 0.7$	1	1.5	$n = 0.7$	1	1.5
0	1.81536	1.78741	1.79013	3.07693	2.95562	3.01639
0.1	1.80080	1.74581	1.71002	3.07692	2.94956	3.00415
0.2	1.79616	1.72536	1.66862	3.08773	2.96177	3.00532
0.3	1.79868	1.71692	1.64606	3.11416	2.99268	3.02004
0.4	1.80750	1.71694	1.63474	3.16042	3.04440	3.05287
0.6	1.84383	1.73702	1.63350	3.33175	3.22400	3.17488
0.8	1.90788	1.78189	1.65280	3.64528	3.51672	3.34473
1	2.00565	1.85331	1.68959	4.11919	3.88741	3.54390

ACKNOWLEDGMENTS

Project funded under the National Recovery and Resilience Plan (NRRP), Mission 4 Component 2 Investment 1.5 - Call for tender No. 3277 of 30/12/2021 of Italian Ministry of University and Research funded by the European Union – NextGenerationEU. Project code ECS00000033, Concession Decree No. 1052 of 23/06/2022 adopted by the Italian Ministry of University and Research, CUP D93C22000460001, "Ecosystem for Sustainable Transition in Emilia-Romagna" (Ecosister), Spoke 4.

AUTHOR DECLARATIONS

Conflict of Interest

The author has no conflicts to disclose.

DATA AVAILABILITY STATEMENT

Data sharing is not applicable to this article as no new data were created or analyzed in this study.

Appendix A: Numerical values of δ_c

Table I lists the eigenvalues computed for converging gravity flow of a power-law fluid in a channel of varying width.

REFERENCES

[1]G. I. Barenblatt and Y. B. Zel'Dovich, "Self-similar solutions as intermediate asymptotics," Annual Review of Fluid Mechanics **4**, 285–312 (1972).
[2]L. I. Sedov, *Similarity and dimensional methods in mechanics* (CRC press, 1993).
[3]S. Longo, *Principles and applications of dimensional analysis and similarity* (Springer, 2021).
[4]J. Gratton and F. Minotti, "Self-similar viscous gravity currents: phase-plane formalism," Journal of Fluid Mechanics **210**, 155–182 (1990).
[5]J. A. Diez, J. Gratton, and F. Minotti, "Self-similar solutions of the second kind of nonlinear diffusion-type equations," Quarterly of Applied Mathematics **50**, 401–414 (1992).
[6]J. A. Diez, R. Gratton, and J. Gratton, "Self-similar solution of the second kind for a convergent viscous gravity current," Physics of Fluids A: Fluid Dynamics **4**, 1148–1155 (1992).
[7]D. G. Aronson and J. Graveleau, "A selfsimilar solution to the focusing problem for the porous medium equation," European Journal of Applied Mathematics **4**, 65–81 (1993).
[8]S. B. Angenent and D. G. Aronson, "The focusing problem for the radially symmetric porous medium equation," Communications in Partial Differential Equations **20**, 1217–1240 (1995).
[9]S. B. Angenent and D. G. Aronson, "Intermediate asymptotics for convergent viscous gravity currents," Physics of Fluids **7**, 223–225 (1995).
[10]D. G. Aronson, J. B. Van Den Berg, and J. Hulshof, "Parametric dependence of exponents and eigenvalues in focusing porous media flows," European Journal of Applied Mathematics **14**, 485 (2003).
[11]Z. Zheng, I. C. Christov, and H. A. Stone, "Influence of heterogeneity on second-kind self-similar solutions for viscous gravity currents," Journal of Fluid Mechanics **747**, 218–246 (2014).
[12]Z. Zheng, S. Shin, and H. A. Stone, "Converging gravity currents over a permeable substrate," Journal of Fluid Mechanics **778**, 669–690 (2015).
[13]J. Gratton and C. A. Perazzo, "Self-similar collapse of a circular cavity of a power-law liquid," Journal of non-Newtonian Fluid Mechanics **165**, 158–162 (2010).
[14]S. Longo, L. Chiapponi, D. Petrolo, A. Lenci, and V. Di Federico, "Converging gravity currents of power-law fluid," Journal of Fluid Mechanics **918**, A5 (2021).
[15]J. Gratton, "Similarity and self similarity in fluid dynamics," Fundamentals of Cosmic Physics **15**, 1–106 (1991).
[16]Z. Zheng and H. A. Stone, "The influence of boundaries on gravity currents and thin films: drainage, confinement, convergence, and deformation effects," Annual Review of Fluid Mechanics **54**, 27–56 (2022).
[17]V. Ciriello, S. Longo, L. Chiapponi, and V. Di Federico, "Porous gravity currents: a survey to determine the joint influence of fluid rheology and variations of medium properties," Advances in Water Resources **92**, 105 – 115 (2016).
[18]W. Ostwald, "Ueber die rechnerische darstellung des strukturgebietes der viskosität," Colloid & Polymer Science **47**, 176–187 (1929).
[19]R. S. Morrell and A. De Waele, *Rubber, resins, paints and varnishes* (Nostrand, 1920).
[20]Wolfram Research, Inc., "Mathematica, Version 11.1," (2017), champaign, IL, 2017.
[21]M. Ungarish, *Gravity Currents and Intrusions: Analysis and Prediction*, Vol. 1 (World Scientific, 2020).
[22]T. V. Ball and H. E. Huppert, "Similarity solutions and viscous gravity current adjustment times," Journal of Fluid Mechanics **874**, 285–298 (2019).